

Deep Learning–Based Pneumonia Classification on Chest X-Ray Images

Mustakim^{1,2,*}, Danur Lestari¹, Hartono³

¹ Department of Information Systems, Faculty of Science and Technology, Universitas Islam Negeri Sultan Syarif Kasim Riau, Pekanbaru, Indonesia

² Department of Computer Science, Faculty of Informatics and Computing, Universiti Sultan Zainal Abidin, Terengganu, Malaysia

³ Department of Mathematics Education, Faculty of Education and Teaching, Universitas Islam Negeri Sultan Syarif Kasim Riau, Pekanbaru, Indonesia

Email: ^{1,*}mustakim@uin-suska.ac.id, ²12150321355@students.uin-suska.ac.id, ³hartono@uin-suska.ac.id

ARTICLE INFORMATION

ARTICLE HISTORY:

Submitted : September 23, 2025

Revised : November 22, 2025

Accept : November 28, 2025

Publish : November 29, 2025

KEYWORD

Convolutional Neural Network;
Deep Learning;
Generative Adversarial Network;
Pneumonia;
Recurrent Neural Network

CORRESPONDENCE AUTHOR

Email: mustakim@uin-suska.ac.id

A B S T R A C T

Pneumonia is a lung infection and one of the leading causes of mortality worldwide. Early and accurate diagnosis is essential to reduce death rates, with chest X-ray (CXR) imaging being the most commonly used diagnostic tool. However, CXR-based pneumonia identification remains challenging due to limited image quality and the shortage of experienced radiologists. To address this issue, this study proposes a hybrid deep learning framework that integrates Convolutional Neural Network (CNN), Recurrent Neural Network (RNN), and Generative Adversarial Network (GAN) to enhance the classification of bacterial and viral pneumonia from CXR images. The dataset comprises 7,927 CXR images, including 3,270 normal cases, 3,001 cases of bacterial pneumonia, and 1,656 cases of viral pneumonia. Four CNN architectures, Xception, InceptionV3, ResNet50V2, and DenseNet201, are evaluated using RMSprop and Stochastic Gradient Descent (SGD) optimizers. Model development and training are conducted using the TensorFlow framework. Experimental results demonstrate that ResNet50V2 with the RMSprop optimizer achieves the highest classification accuracy of 0.85, while also yielding the fastest training time of 2,215 seconds. These findings indicate that the proposed approach can support faster and more accurate pneumonia screening, particularly in healthcare facilities with limited diagnostic resources.

1. INTRODUCTION

Pneumonia is a lung infection caused by various pathogens, such as bacteria, viruses, and fungi [1]. This disease causes inflammation in the lung parenchyma, particularly the alveoli, which play a crucial role in gas exchange. Inflammation can lead to fluid or pus filling the alveoli, resulting in symptoms such as shortness of breath, coughing, chest pain, and fever [3]. Pneumonia is one of the leading causes of death worldwide, particularly among vulnerable groups such as children under the age of five and elderly individuals over 65 years old [4]. According to the World Health Organization (WHO), pneumonia accounted for 14% of deaths among children under five years old in 2019 [5], [6]. Additionally, the COVID-19 pandemic caused by the SARS-CoV-2 virus has led to an increase in pneumonia cases requiring intensive care in hospitals, placing a burden on healthcare systems worldwide [7], [8].

Early detection and accurate diagnosis are crucial in reducing pneumonia-related mortality [3], [6]. One of the primary methods used for pneumonia diagnosis is medical imaging through Chest X-Ray (CXR) [9], [10]. Although CXR is a more economical, faster, and lower-radiation diagnostic tool compared to Computed Tomography (CT) scans and Magnetic Resonance Imaging (MRI) [11], [12], its resolution limitations often make it difficult to distinguish pneumonia from other lung conditions [13], [14]. Moreover, pneumonia identification through CXR relies on radiologists' expertise, whereas the number of radiology specialists available, especially in developing countries, remains very limited [4], [13]. Therefore, integrating AI into medical image interpretation has become a promising alternative to assist radiologists.

With the advancement of technology, Deep Learning (DL)-based methods have become a potential solution for assisting pneumonia diagnosis through automated CXR analysis [15]. DL offers a data-driven approach that allows systems to learn directly from images without requiring manual feature extraction, as in traditional Machine Learning methods [16]. One of the most commonly used DL algorithms in medical image analysis is Convolutional Neural Network (CNN) [17], [18], which can recognize complex patterns in radiographic images and classify diseases with high accuracy without the need for manual feature extraction, unlike traditional Machine Learning methods [19].

Although CNN has proven effective in classifying lung diseases [20], one of the main challenges in implementing this model is the limited availability of high-quality medical datasets [3]. Small or imbalanced datasets can lead to issues such as overfitting and poor generalization to new data [21], [22]. To overcome this limitation, Generative Adversarial Networks (GAN) have been used to improve the quality and quantity of training data [20]. GANs consist of two neural networks: a generator that creates synthetic images resembling real data and a discriminator that distinguishes between real and generated images [4], [23]. Using this approach, GANs can generate realistic synthetic CXR images to enhance datasets and improve CNN model performance in pneumonia detection [24]. Previous studies have shown that GAN-



based data augmentation techniques can address dataset imbalance issues and enhance the accuracy of DL-based disease classification models [20], [25].

In addition to CNN and GAN, this study also utilizes Recurrent Neural Networks (RNN) to improve the accuracy of pneumonia classification based on CXR images. RNN is a type of artificial neural network designed to handle sequential data by considering information from previous steps in the current computation [26], [27]. The RNN processes sequential feature vectors extracted from different image regions by CNN. One commonly used RNN variant in medical applications is Long Short-Term Memory (LSTM) and Gated Recurrent Unit (GRU), which are designed to address the vanishing gradient problem often found in standard RNNs [28]. LSTM and GRU allow the model to store and utilize long-term information, which is useful in analyzing disease patterns based on medical imaging data [28], [29].

In this study, CNN is used to extract features from CXR images, while RNN (LSTM or GRU) processes and recognizes patterns from the extracted features. RNN plays a role in capturing the correlation between image features generated by CNN from different parts of the image, enabling the model to understand more complex patterns in disease distribution. [30], [31]. This combination enables the model to better understand complex relationships within medical imaging data, thereby enhancing pneumonia detection capabilities [32]. Previous studies have shown that integrating CNN and RNN can improve disease classification accuracy, especially in image-based and sequential medical data applications [33], [34].

Several previous studies have implemented various CNN architectures for pneumonia classification using CXR [35]. For instance, study [6] classified bacterial and viral pneumonia by evaluating the effectiveness of four CNN architectures: Xception, InceptionV3, ResNet50V2, and DenseNet201. This study compared model performance using two optimization methods, RMSprop and SGD. The results showed that ResNet50V2, when paired with the RMSprop optimizer, achieved the highest classification accuracy of 0.83 and the fastest processing time of 2,460 seconds [6]. However, most studies only compare one or two architectures without evaluating multiple models simultaneously [36]. Furthermore, study [37] proposed the use of class-specific GANs for pneumonia classification. This study found that class-based GANs generated high-quality images, helping to reduce the risk of overfitting and improving CNN model accuracy in pneumonia classification. Another study by [27] combined CNN and RNN for detecting lung diseases, including COVID-19 and pneumonia. This study found that integrating ResNet152V2 with a Gated Recurrent Unit (GRU) achieved the highest accuracy of 93.37%, indicating that CNN-RNN integration can enhance the accuracy of lung disease detection. Study [38] combined two datasets consisting of 180 and 6,054 CXR images of COVID-19 and pneumonia with 8,851 normal CXR images, proposing the Xception and ResNet50V2 architectures, which achieved an accuracy of 91.4%. Study [39] applied K-Fold Cross Validation on ResNet-50 with the SGD optimizer and used 15,143 X-ray images with a resolution of 224x224 pixels, achieving an accuracy of 99%. Study [40] implemented a CNN algorithm using ResNet50 and obtained a peak accuracy of 98.6%. Study [41] used the InceptionV3 model to detect pneumonia from chest X-ray images, achieving an accuracy of 92.8%. Study [42] trained 5,247 chest X-ray images using the DenseNet201 architecture and achieved an accuracy of 93.3%. Therefore, this research focuses on comparing four popular architectures in pneumonia classification—Xception, InceptionV3, ResNet50V2, and DenseNet201—to identify the best model for CXR-based diagnosis. Additionally, this study evaluates the impact of two types of optimizers, RMSprop and SGD, on model accuracy and efficiency in pneumonia detection.

This study aims to analyze and compare the performance of four architectures in pneumonia classification using CXR images, evaluate the impact of two types of optimizers on model accuracy and efficiency, and explore the use of GAN as a data augmentation method to improve dataset quality. Additionally, this research examines the effectiveness of combining CNN and RNN for pneumonia classification, with the expectation that this approach can enhance the performance of DL-based diagnostic models. With this approach, the study seeks to identify the best combination of CNN architecture, RNN type, and optimizer that can be applied in DL-based diagnostic systems, particularly in healthcare facilities with limited radiology experts. The novelty of this research lies in its more comprehensive comparative approach compared to previous studies, as it not only compares various CNN architectures and optimizers but also integrates GAN to enhance training data quality and explores the use of RNN to improve pneumonia classification performance. Thus, this study contributes to the development of more accurate and efficient DL models that can be implemented in healthcare systems to assist radiologists in diagnosing pneumonia more quickly and accurately.

2. RESEARCH METHODOLOGY

2.1 Research Stages

This research is presented in a more structured and objective manner through a flowchart Figure 1, illustrating each stage from collecting data to evaluation.

2.2 Collecting Data

The CXR image dataset used in this study is accessible through the Mendeley Dataset platform, owned by [43]. This dataset consists of three classes: Normal, Bacterial Pneumonia, and Viral Pneumonia, with 3,270, 3,001, and 1,656 images, respectively. In total, the dataset comprises 7,927 CXR images [6]. Table I provides details on the number of CXR images in each category. Figure 2 illustrates the CXR dataset used.



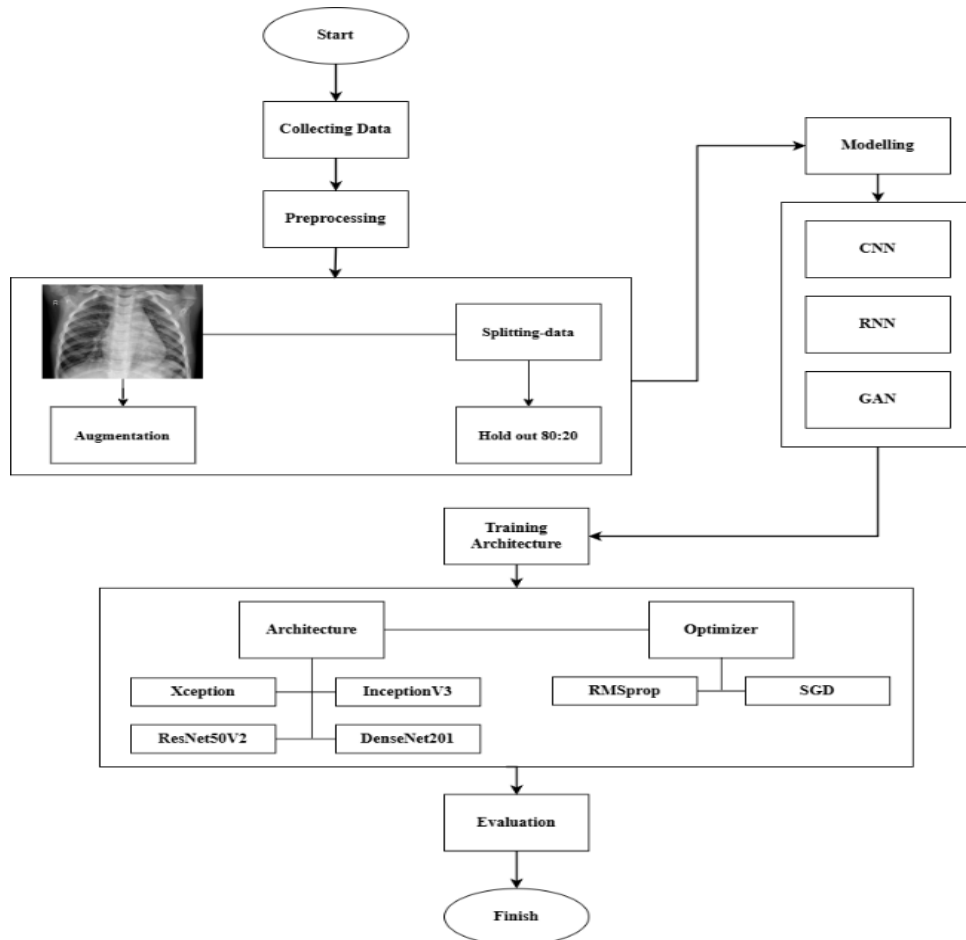


Figure 1. Research Method

Table 1. Details of the CXR dataset

Type	Number of Datasets
Normal	3270
Bacterial Pneumonia	3001
Viral Pneumonia	1656
Total	7927

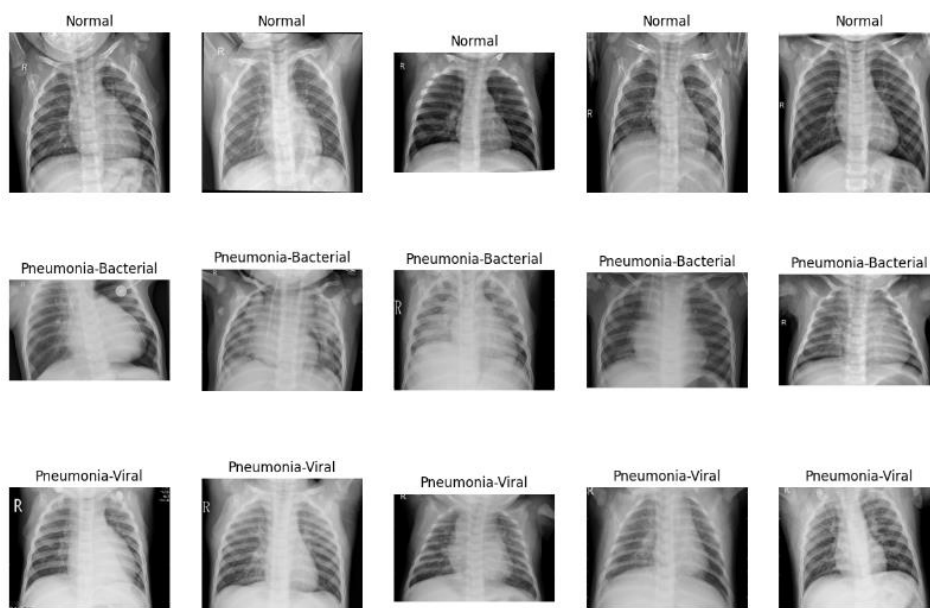


Figure 2. CXR dataset

2.3 Preprocessing and Data Augmentation

During the data processing stage, all CXR images were resized to a uniform dimension of 224x224 pixels to ensure consistency in analysis. Additionally, data augmentation was performed by applying a 45-degree rotation to enhance the diversity of features recognizable by the model, as shown in Fig 1. Augmentation techniques such as rotation are commonly used in medical image processing research to improve model robustness against variations in imaging data [33]. Data preprocessing, model implementation, and training were performed using the TensorFlow framework with the Keras API. This framework supports efficient optimization of CNN, RNN, and GAN models and ensures reproducible experiments for medical image classification.

Next, the hold-out method was applied to split the dataset, using an 80:20 ratio to separate the data into training and validation sets. This approach is commonly used in deep learning studies as it balances the size of training and validation data, optimizing the model's learning process while minimizing the risk of overfitting [28]. Evaluating the model with this proportion allows for a comprehensive assessment of its performance, providing more accurate insights into the model's effectiveness in recognizing patterns in CXR images [35].

2.4. Modeling

2.4.1 Convolutional Neural Network

Convolutional Neural Networks (CNN) are neural networks designed to process images by recognizing patterns like the human brain. CNN has key layers: convolutional layers for feature extraction, pooling layers to reduce data size, and fully connected layers for classification. CNN's strengths include automatic feature extraction, robustness to object position and rotation, and transfer learning, which enables using pre-trained models like VGG16, ResNet, and DenseNet for better performance [44], [45].

In the field of medical imaging, CNN has been successfully applied for breast cancer detection, brain tumor segmentation, and lung disease diagnosis through CXR image analysis [46]. However, CNNs have limitations, such as the need for large datasets to prevent overfitting and high computational demands due to a large number of parameters. Additionally, deeper CNN models often suffer from the vanishing gradient problem, which can be addressed using residual networks (ResNet) [47]. Despite these challenges, CNN remains a highly effective method for medical image analysis and various other computer vision applications.

In general, CNN has a structure consisting of several main layers: the convolutional layer, the activation layer, the pooling (subsampling) layer, and the fully connected layer, with the general equations as equations 1-4.

$$Y(i, j) = \sum_m X(i - m, j - n)K(m, n) \quad (1)$$

$$f(x) = \max(0, x) \quad (2)$$

$$Y(i, j) = \max(m, n) X(2i + m, 2j + n) \quad (3)$$

$$Y = WX + b \quad (4)$$

2.4.2 Recurrent Neural Network

Recurrent Neural Networks (RNNs) are a type of artificial neural network designed to process sequential data, such as text, audio, and time-series signals. Unlike feedforward neural networks, RNNs have an internal memory that allows previous information to be used in the current processing step, making them suitable for tasks such as natural language processing (NLP) and time-series analysis [31], [33]. In this study, the CNN models are trained using a defined learning rate (η) to control the magnitude of weight updates, dropout (p) to reduce overfitting by randomly deactivating neurons, and the ReLU activation function to introduce nonlinearity. The learning process is optimized by minimizing a loss function $L(y, y')$, where y represents the true label and y' denotes the predicted output. All mathematical formulations are explicitly annotated to clarify the role of each parameter, ensuring ease of understanding and reproducibility.

The RNN architecture consists of recurrent layers, where the output from one time step serves as input for the next. However, this model often suffers from the vanishing gradient problem, which hampers long-term learning. To address this issue, variants such as Long Short-Term Memory (LSTM) and Gated Recurrent Unit (GRU) were developed, enabling more effective handling of long-term dependencies [28], [34]. RNNs are widely used in applications such as speech recognition, automatic translation, and financial forecasting, but they have limitations in computational efficiency due to their sequential nature, which makes parallelization challenging [34]. RNN works by updating the hidden state based on the current input and the previous hidden state.

$$h_t = f(W_h h_{t-1} + W_x x_t + b_h) \quad (5)$$

2.4.3 Generative Adversarial Networks

Generative Adversarial Networks (GANs) are a type of artificial neural network used to generate new data similar to real data. GANs consist of two main networks: the Generator, which creates synthetic data, and the Discriminator, which distinguishes between real and generated data. These networks are trained simultaneously in a competitive process, where the Generator continuously improves the quality of its generated data to make it harder for the Discriminator to



differentiate. [20]. GAN has been used in various applications, such as generating realistic images, enhancing the resolution of medical images, simulating data for DL model training, and deepfake generation [37]. Several GAN variants have been developed to improve training stability and output quality, including Deep Convolutional GAN (DCGAN), Wasserstein GAN (WGAN), and StyleGAN [48]. However, GANs face challenges such as mode collapse, where the Generator produces only a limited variation of data, and convergence difficulties due to the complex dynamics of the training process [49].

$$G(z, \theta_G) \quad (6)$$

$$D(x, \theta_D) \quad (7)$$

In this study, GAN-generated synthetic CXR images are used as data augmentation to increase training data diversity and balance class distribution. The augmented dataset is combined with original images to train the CNN models, improving feature generalization and classification performance, particularly for underrepresented pneumonia classes.

2.4 Training Architecture

In Deep Learning, various neural network architectures have been developed to enhance image classification performance, particularly on large datasets such as ImageNet. Some commonly used models include Xception, InceptionV3, ResNet50V2, and DenseNet201, each offering advantages in processing efficiency and feature extraction. Xception is an improvement over Inception that utilizes depthwise separable convolutions, increasing processing efficiency without reducing accuracy [50].

In contrast, InceptionV3 leverages Inception modules, allowing multi-scale feature extraction within a single convolutional stage, while also employing factorized convolutions and batch normalization to enhance training stability [51]. ResNet50V2 introduces the concept of residual connections, which help deeper networks overcome the vanishing gradient problem, leading to more stable training [38]. Meanwhile, DenseNet201 features a unique structure that connects each layer to all subsequent layers, enabling more efficient feature reuse and reducing the number of required parameters, making it more efficient and resistant to overfitting [42].

These four models are often used in combination with Transfer Learning, where pre-trained models on large datasets such as ImageNet can be fine-tuned for new datasets. This approach is particularly beneficial in medical imaging and computer vision applications, as it improves accuracy without requiring extremely large datasets or long training times [52]. With these advanced architectures, Deep Learning continues to evolve as a powerful tool for various image classification and visual analysis tasks.

To further analyze these architectures, an architectural comparison is conducted in terms of parameter count, computational complexity (FLOPs), and power efficiency, as summarized in an article [35]. The four models are selected because they are widely adopted, experimentally stable, and offer a balanced trade-off between accuracy and computational efficiency, making them suitable for medical image classification tasks.

2.5 Optimizer

In Deep Learning, choosing the right optimizer is key to fast and efficient training. Two common optimizers are Stochastic Gradient Descent (SGD) and RMSprop. SGD updates model weights using small data batches (mini-batch), making training faster and using less memory than full batch gradient descent. However, it can be unstable, causing slow convergence or getting stuck in local minima. [53].

To improve stability and efficiency, various SGD variants have been developed, such as SGD with momentum, which helps maintain the optimization direction based on previous gradients, thereby preventing excessive oscillations [54]. On the other hand, RMSprop (Root Mean Square Propagation) is an optimizer that adaptively adjusts the learning rate for each parameter by considering the exponential moving average of past squared gradients. This approach helps address the vanishing gradient problem and enables more stable learning, particularly in deeper networks such as CNNs and RNNs [55].

2.6 Evaluation

In this study, model evaluation was conducted based on two key metrics: accuracy and processing time. Accuracy is the primary metric for assessing the performance of a classification model, calculated as the percentage of correct predictions relative to the total number of tested data. A high accuracy indicates that the model can classify data effectively, while a low accuracy suggests the need for improvements in the training process or model architecture selection [48].

In addition to accuracy, processing time is an essential factor in evaluating model efficiency, especially in real-time applications or environments with limited computational resources. More complex architectures tend to have longer processing times, making it necessary to balance accuracy and time efficiency [9]. In this study, the combination of these two metrics was used to assess the overall model performance. A model with high accuracy but significantly long processing time may be impractical, while a model with fast processing time but low accuracy is also ineffective. Therefore, selecting the optimal model depends on the trade-off between these two factors, tailored to the requirements of the intended application [56].



3. RESULT AND DISCUSSION

The training process for the Xception, InceptionV3, ResNet50V2, and DenseNet201 models started with pre-trained weights from ImageNet, a common dataset for image classification. The base models were loaded without the top classification layer and set to 224×224×3 input size, ensuring they retained their learned features while staying non-trainable during training. To prevent overfitting, a dropout layer (0.2) was added. The final layer used a softmax activation function with three output neurons, corresponding to Normal, Bacterial Pneumonia, and Viral Pneumonia classifications. The dataset, sourced from Mendeley, contained 7,927 images, divided into 3,270 Normal, 3,001 Bacterial Pneumonia, and 1,656 Viral Pneumonia cases. During the training process, parameter configuration played a crucial role in determining the model's performance. The key parameters used in this study are presented in Table 2.

Table 2. Details of the parameters used

Parameter	Value
Drop Out	0.2
Hold-Out	80:20:00
Epoch	50
Batch Size	128
Learning Rate	0.0001
Optimizer	RMSprop, SGD

To improve classification accuracy, this study implements three main approaches in Deep Learning: CNN for feature extraction and classification, RNN for handling possible sequential patterns in medical images, and GAN as a data augmentation method to balance the number of samples in each class. The models were tested using two optimizers: RMSprop, which helps stabilize weight updates during training, and SGD, which plays a role in improving model generalization. The accuracy results and model performance evaluation based on training time for architectures trained with both optimizers are summarized in Table 3 and Table 4.

Table 3. Training accuracy results

Architectures	CNN		RNN		GAN	
	RMSprop	SGD	RMSprop	SGD	RMSprop	SGD
Xception	0,83	0,75	0,83	0,55	0,85	0,79
InceptionV3	0,74	0,71	0,84	0,72	0,85	0,79
ResNet50V2	0,83	0,71	0,85	0,73	0,82	0,71
DenseNet201	0,83	0,8	0,83	0,68	0,81	0,82

Table 4. Details of the CXR dataset

Architectures	CNN		RNN		GAN	
	RMSprop	SGD	RMSprop	SGD	RMSprop	SGD
Xception	4194	6278	3800	5497	1119	5360
InceptionV3	6444	5604	2586	4972	3129	5659
ResNet50V2	2460	6320	2215	5306	2579	4998
DenseNet201	3220	6154	2571	6121	3349	2304

Table 3 presents the training accuracy results for various model architectures using RMSprop and SGD optimizers. In the CNN model, ResNet50V2, DenseNet201, and Xception achieved the highest accuracy (0.83) with RMSprop, while InceptionV3 had the lowest accuracy (0.74). In the RNN model, ResNet50V2 with RMSprop recorded the highest accuracy (0.85), whereas Xception with SGD had the lowest accuracy (0.55). In the GAN model, Xception with RMSprop achieved the highest accuracy (0.85), while InceptionV3 with SGD had the lowest accuracy (0.71). Overall, RMSprop provided better accuracy results compared to SGD. The comparison of overall accuracy across different architectures and optimizers is shown in figure 3.

RMSprop generally yields higher accuracy because its adaptive learning rate adjusts weight updates based on recent gradient magnitudes, leading to more stable and faster convergence. This mechanism helps prevent oscillations during training, especially in deep architectures. However, faster convergence may increase the risk of overfitting, while training time variations reflect differences in model complexity and optimization dynamics.

Table 4 presents the training time in seconds. In the CNN model, ResNet50V2 with RMSprop was the fastest (2,460 seconds), while InceptionV3 with RMSprop required the longest time (6,444 seconds). In the RNN model, ResNet50V2 with RMSprop was again the fastest (2,215 seconds), whereas Xception with SGD took the longest time (5,497 seconds). For the GAN model, Xception with RMSprop had the shortest training time (1,119 seconds), while DenseNet201 with RMSprop was the slowest (3,349 seconds).

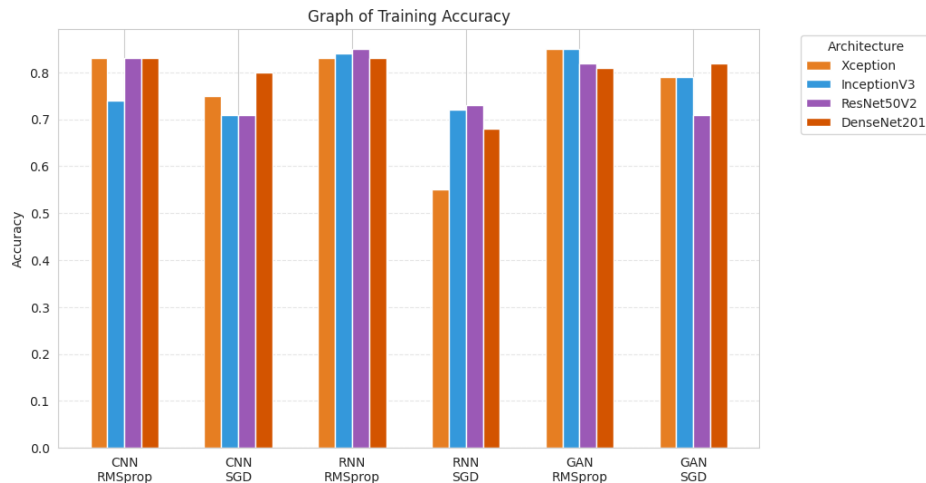


Figure 3. Training accuracy graph

Thus, ResNet50V2 with RMSprop is the best choice for CNN and RNN in terms of time efficiency, while Xception with RMSprop performs best in the GAN model. The overall comparison of model performance evaluation based on training time across different architectures and optimizers is shown in Figure 4.

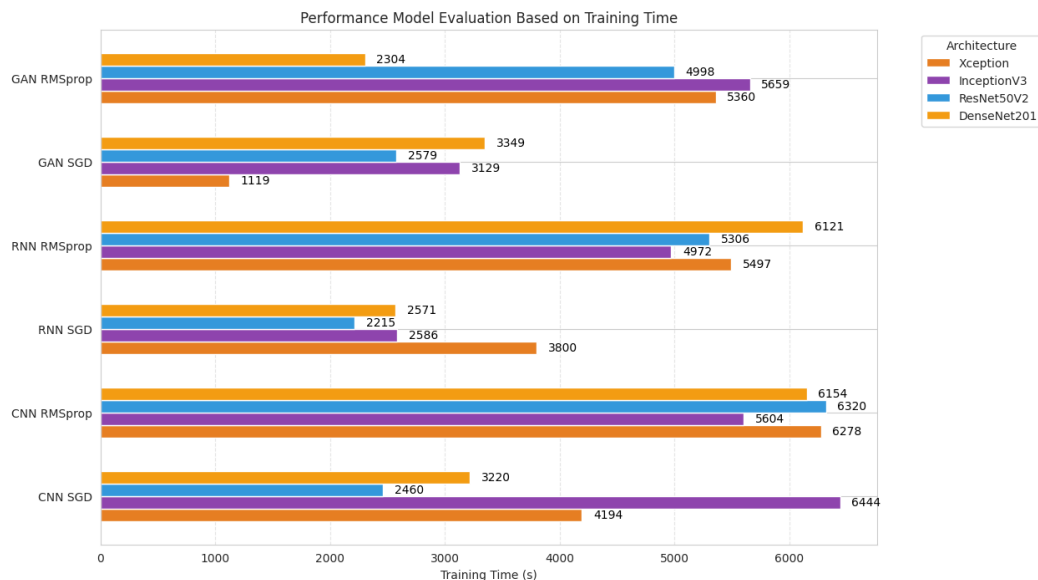


Figure 4. Performance model evaluation based on training time

4. CONCLUSION

This study examines the combination of deep learning models—CNN, RNN, and GAN—with four architectures (Xception, InceptionV3, ResNet50V2, DenseNet201) and two optimizers (RMSprop and SGD) for classifying pneumonia based on CXR images. The results show that RMSprop consistently outperforms SGD in terms of accuracy. ResNet50V2 with RMSprop is the best combination for CNN and RNN models, while Xception with RMSprop is optimal for the GAN model. This approach evaluates not only accuracy but also processing efficiency, with the RNN-ResNet50V2-RMSprop combination achieving the highest accuracy (0.85) and a processing time of 2,215 seconds. The novelty of this research lies in integrating CNN, RNN, and GAN methods, enabling sequential information processing and addressing data imbalance using GAN. The novelty of this study is in the integration of CNN, RNN, and GAN methods, which facilitate sequential information processing and handle data imbalance. In terms of creativity, the unique combination of CNN architectures and the exploration of optimization techniques enhance model performance. The technical depth is reflected in the analysis, which considers not only accuracy but also processing efficiency. The application of this model has the potential to improve early detection and accelerate diagnosis, particularly in areas with limited medical resources. However, successful implementation requires collaboration between research institutions, policymakers, and healthcare providers. Future research should focus on improving feature representation and model robustness by integrating attention mechanisms or transformer-based architectures into the proposed framework. Additionally, expanding the dataset with

multi-center CXR data and evaluating real-time clinical deployment could further enhance generalization performance and practical applicability.

REFERENCES

- [1] A. U. Ibrahim, M. Ozsoz, S. Serte, F. Al-Turjman, and P. S. Yakoi, "Pneumonia classification using deep learning from chest X-ray images during COVID-19," *Cognit Comput*, pp. 1–13, 2021. doi: 10.1007/s12559-020-09787-5
- [2] R. Siddiqi and S. Javaid, "Deep Learning for Pneumonia Detection in Chest X-ray Images: A Comprehensive Survey," Aug. 01, 2024, *Multidisciplinary Digital Publishing Institute (MDPI)*. doi: 10.3390/jimaging10080176.
- [3] W. Khan, N. Zaki, and L. Ali, "Intelligent pneumonia identification from chest x-rays: A systematic literature review," *IEEE Access*, vol. 9, pp. 51747–51771, 2021. doi: 10.1109/ACCESS.2021.3069937
- [4] S. Sharma and K. Guleria, "A Deep Learning based model for the Detection of Pneumonia from Chest X-Ray Images using VGG-16 and Neural Networks," in *Procedia Computer Science*, Elsevier B.V., 2022, pp. 357–366. doi: 10.1016/j.procs.2023.01.018.
- [5] D. Lestari, "Classification of Bacterial and Viral Pneumonia Using Chest X-Ray Images with Convolutional Neural Network," in *2024 International Conference on Decision Aid Sciences and Applications (DASA)*, IEEE, 2024, pp. 1–6. doi: 10.1109/DASA63652.2024.10836528
- [6] D. Chittora, B. R. Meena, S. Mittholiya, and K. Sharma, "Updates of COVID-19," *Research on Biomedical Engineering*, vol. 37, no. 4, pp. 835–848, 2021. doi: 10.1007/s42600-021-00140-9
- [7] H. Rossman *et al.*, "Hospital load and increased COVID-19 related mortality in Israel," *Nat Commun*, vol. 12, no. 1, p. 1904, 2021. doi: 10.1038/s41467-021-22214-z
- [8] M. Yaseliani, A. Z. Hamadani, A. I. Maghsoodi, and A. Mosavi, "Pneumonia detection proposing a hybrid deep convolutional neural network based on two parallel visual geometry group architectures and machine learning classifiers," *IEEE access*, vol. 10, pp. 62110–62128, 2022. doi: 10.1109/ACCESS.2022.3182498
- [9] D. Schaudt *et al.*, "A Critical Assessment of Generative Models for Synthetic Data Augmentation on Limited Pneumonia X-ray Data," *Bioengineering*, vol. 10, no. 12, p. 1421, 2023. doi: 10.3390/bioengineering10121421
- [10] X. Wang, Y. Peng, L. Lu, Z. Lu, M. Bagheri, and R. M. Summers, "Chestx-ray8: Hospital-scale chest x-ray database and benchmarks on weakly-supervised classification and localization of common thorax diseases," in *Proceedings of the IEEE conference on computer vision and pattern recognition*, 2017, pp. 2097–2106.
- [11] M. Mardani *et al.*, "Deep generative adversarial neural networks for compressive sensing MRI," *IEEE Trans Med Imaging*, vol. 38, no. 1, pp. 167–179, 2018. doi: 10.1109/TMI.2018.2858752
- [12] R. Siddiqi, "Efficient pediatric pneumonia diagnosis using depthwise separable convolutions," *SN Comput Sci*, vol. 1, no. 6, p. 343, 2020. doi: 10.1007/s42979-020-00361-2
- [13] E. Çalli, E. Sogancioglu, B. van Ginneken, K. G. van Leeuwen, and K. Murphy, "Deep learning for chest X-ray analysis: A survey," *Med Image Anal*, vol. 72, p. 102125, 2021. doi: 10.1016/j.media.2021.102125
- [14] F. Al-Turjman, *AI-powered IoT for COVID-19*. CRC Press, 2020.
- [15] X. Zhou, P. Lu, Z. Zheng, D. Tolliver, and A. Keramati, "Accident prediction accuracy assessment for highway-rail grade crossings using random forest algorithm compared with decision tree," *Reliab Eng Syst Saf*, vol. 200, p. 106931, 2020. doi: 10.1016/j.res.2020.106931
- [16] S. Kumar and S. Prakash, "Pneumonia Identification and Classification Using CNN Model Based on Chest X-Ray Image in Healthcare," in *International Conference on Advanced Computing and Intelligent Engineering*, Springer, 2022, pp. 473–486. doi: 10.1007/978-981-99-5015-7_40
- [17] D. Hastari, S. Winanda, A. R. Pratama, N. Nurhaliza, and E. S. Ginting, "Application of Convolutional Neural Network ResNet-50 V2 on Image Classification of Rice Plant Disease," *Public Research Journal of Engineering, Data Technology and Computer Science*, vol. 1, no. 2, 2024. doi: 10.57152/predatecs.v1i2.865
- [18] R. Yamashita, M. Nishio, R. K. G. Do, and K. Togashi, "Convolutional neural networks: an overview and application in radiology," *Sights Imaging*, vol. 9, pp. 611–629, 2018. doi: 10.1007/s13244-018-0639-9
- [19] S. Motamed, P. Rogalla, and F. Khalvati, "Data augmentation using Generative Adversarial Networks (GANs) for GAN-based detection of Pneumonia and COVID-19 in chest X-ray images," *Inform Med Unlocked*, vol. 27, p. 100779, 2021. doi: 10.1016/j.imu.2021.100779
- [20] Y.-D. Zhang *et al.*, "Image based fruit category classification by 13-layer deep convolutional neural network and data augmentation," *Multimed Tools Appl*, vol. 78, pp. 3613–3632, 2019. doi: 10.1007/s11042-017-5243-3
- [21] R. Hao, K. Namdar, L. Liu, M. A. Haider, and F. Khalvati, "A comprehensive study of data augmentation strategies for prostate cancer detection in diffusion-weighted MRI using convolutional neural networks," *J Digit Imaging*, vol. 34, pp. 862–876, 2021. doi: 10.1007/s10278-021-00478-7
- [22] I. Goodfellow *et al.*, "Generative adversarial nets," *Adv Neural Inf Process Syst*, vol. 27, 2014.
- [23] A. Makhlof, M. Maayah, N. Abughanam, and C. Catal, "The use of generative adversarial networks in medical image augmentation," *Neural Comput Appl*, vol. 35, no. 34, pp. 24055–24068, 2023. doi: 10.1007/s00521-023-09100-z
- [24] D. Srivastav, A. Bajpai, and P. Srivastava, "Improved classification for pneumonia detection using transfer learning with GAN based synthetic image augmentation," in *2021 11th international conference on cloud computing, data science & engineering (confluence)*, IEEE, 2021, pp. 433–437. doi: 10.1109/Confluence51648.2021.9377062
- [25] J. Zhang, Y. Zeng, and B. Starly, "Recurrent neural networks with long term temporal dependencies in machine tool wear diagnosis and prognosis," *SN Appl Sci*, vol. 3, no. 4, p. 442, 2021. doi: 10.1007/s42452-021-04427-5
- [26] I. Kanjanasurat, K. Tenghongsakul, B. Purahong, and A. Lasakul, "CNN–RNN network integration for the diagnosis of COVID-19 using chest X-ray and CT images," *Sensors*, vol. 23, no. 3, p. 1356, 2023. doi: 10.3390/s23031356



- [27] A. Makandar and M. N. Jadhav, "Disease Recognition in Medical Images Using CNN-LSTM-GRU Ensemble, a Hybrid Deep Learning," in *2023 7th International Conference on Computation System and Information Technology for Sustainable Solutions (CSITSS)*, IEEE, 2023, pp. 1–9. doi: 10.1109/CSITSS60515.2023.10334080
- [28] A. A. Wafa, R. M. Essa, A. A. Abohany, and H. E. Abdelkader, "Integrating deep learning for accurate gastrointestinal cancer classification: a comprehensive analysis of MSI and MSS patterns using histopathology data," *Neural Comput Appl*, pp. 1–33, 2024. doi: 10.1007/s00521-024-10287-y
- [29] S. Lafraxo, M. El Ansari, and L. Koutti, "A new hybrid approach for pneumonia detection using chest X-rays based on ACNN-LSTM and attention mechanism," *Multimed Tools Appl*, pp. 1–23, 2024. doi: 10.1007/s11042-024-18401-x
- [30] R. Karla and R. Yalavarthi, "A Hybrid RNN-based Deep Learning Model for Lung Cancer and COPD Detection," *Engineering, Technology and Applied Science Research*, vol. 14, no. 5, pp. 16847–16853, Oct. 2024, doi: 10.48084/etasr.8181.
- [31] M. Kavitha, K. Vidhya, S. Sreeja, G. Roopashri, and P. Muhil, "Automated lung disease detection, classification and prediction using RNN framework," in *E3S Web of Conferences*, EDP Sciences, Feb. 2024. doi: 10.1051/e3sconf/202449103015.
- [32] Y. Lu *et al.*, "A hybrid CNN-RNN approach for survival analysis in a Lung Cancer Screening study," *Heliyon*, vol. 9, no. 8, Aug. 2023, doi: 10.1016/j.heliyon.2023.e18695.
- [33] M. M. Islam, M. Z. Islam, A. Asraf, M. S. Al-Rakhami, W. Ding, and A. H. Sodhro, "Diagnosis of COVID-19 from X-rays using combined CNN-RNN architecture with transfer learning," *BenchCouncil Transactions on Benchmarks, Standards and Evaluations*, vol. 2, no. 4, Oct. 2022, doi: 10.1016/j.tbench.2023.100088.
- [34] A. Mahadar, P. Mangukiya, and T. Baraskar, "Comparison and Evaluation of CNN Architectures for Classification of Covid-19 and Pneumonia," in *2021 Sixth International Conference on Image Information Processing (ICIIP)*, IEEE, 2021, pp. 110–115. doi: 10.1109/ICIIP53038.2021.9702676
- [35] B. Nugroho and A. Yuniarti, "Performance of root-mean-square propagation and adaptive gradient optimization algorithms on covid-19 pneumonia classification," in *2022 IEEE 8th Information Technology International Seminar (ITIS)*, IEEE, 2022, pp. 333–338. doi: 10.1109/ITIS57155.2022.10010119
- [36] D. Kalra, V. Khare, and R. Kumar, "Class-Specific GANs to Improve Synthesis of Bacterial and Viral Pneumonia Chest X-Ray Images," *Journal Européen des Systèmes Automatisés*, vol. 57, no. 6, p. 1817, 2024.
- [37] M. Rahimzadeh and A. Attar, "A modified deep convolutional neural network for detecting COVID-19 and pneumonia from chest X-ray images based on the concatenation of Xception and ResNet50V2," *Inform Med Unlocked*, vol. 19, Jan. 2020, doi: 10.1016/j.imu.2020.100360.
- [38] Susanti, Mustakim, R. Novita, and I. Permana, "Application of Residual Network Architecture on Covid-19 Chest x-ray Classification," in *2022 International Symposium on Information Technology and Digital Innovation (ISITDI)*, 2022, pp. 121–125. doi: 10.1109/ISITDI55734.2022.9944525.
- [39] S. T. Rizaldi, Mustakim, I. Permana, and M. Afdal, "Image Enhancement on Deep Learning Algorithm for COVID-19 Lung X-Ray Classification," in *2022 International Symposium on Information Technology and Digital Innovation (ISITDI)*, 2022, pp. 11–15. doi: 10.1109/ISITDI55734.2022.9944501.
- [40] M. M. Hasan, M. M. J. Kabir, M. R. Haque, and M. Ahmed, "A combined approach using image processing and deep learning to detect pneumonia from chest X-ray image," in *2019 3rd international conference on electrical, Computer & Telecommunication Engineering (ICECTE)*, IEEE, 2019, pp. 89–92. doi: 10.1109/ICECTE48615.2019.9303543
- [41] T. Rahman *et al.*, "Transfer learning with deep convolutional neural network (CNN) for pneumonia detection using chest X-ray," *Applied Sciences*, vol. 10, no. 9, p. 3233, 2020. doi: 10.3390/app10093233
- [42] U. Sait *et al.*, "Curated dataset for covid-19 posterior-anterior chest radiography images (x-rays)," *Mendeley Data*, vol. 1, no. J, 2020. doi:10.17632/9xkhgts2s6.1
- [43] K. He, X. Zhang, S. Ren, and J. Sun, "Identity mappings in deep residual networks," in *Computer Vision—ECCV 2016: 14th European Conference, Amsterdam, The Netherlands, October 11–14, 2016, Proceedings, Part IV 14*, Springer, 2016, pp. 630–645. doi: 10.1007/978-3-319-46493-0_38
- [44] P. D. Rinanda, D. N. Aini, T. A. Pertiwi, S. Suryani, and A. J. Prakash, "Implementation of Convolutional Neural Network (CNN) for Image Classification of Leaf Disease In Mango Plants Using Deep Learning Approach," *Public Research Journal of Engineering, Data Technology and Computer Science*, vol. 1, no. 2, pp. 56–61, Feb. 2024, doi: 10.57152/predatecs.v1i2.872.
- [45] F. Zheng *et al.*, "Accurately Discriminating COVID-19 from Viral and Bacterial Pneumonia According to CT Images Via Deep Learning," *Interdiscip Sci*, vol. 13, no. 2, pp. 273–285, Jun. 2021, doi: 10.1007/s12539-021-00420-z.
- [46] G. Huang, Z. Liu, L. Van Der Maaten, and K. Q. Weinberger, "Densely connected convolutional networks," in *Proceedings of the IEEE conference on computer vision and pattern recognition*, 2017, pp. 4700–4708.
- [47] S. Vashisht, S. Lamba, B. Sharma, and A. Sharma, "Pneumonia classification using CNN-GAN," in *2023 International Conference on Sustainable Computing and Data Communication Systems (ICSCDS)*, IEEE, 2023, pp. 456–461. doi: 10.1109/ICSCDS56580.2023.10104733
- [48] D. Srivastav, A. Bajpai, and P. Srivastava, "Improved classification for pneumonia detection using transfer learning with gan based synthetic image augmentation," in *2021 11th International Conference on Cloud Computing, Data Science & Engineering (Confluence)*, IEEE, 2021, pp. 433–437. doi: 10.1109/Confluence51648.2021.9377062
- [49] F. Chollet, "Xception: Deep learning with depthwise separable convolutions," in *Proceedings of the IEEE conference on computer vision and pattern recognition*, 2017, pp. 1251–1258.
- [50] N. S. Shadin, S. Sanjana, and N. J. Lisa, "COVID-19 diagnosis from chest X-ray images using convolutional neural network (CNN) and InceptionV3," in *2021 International conference on information technology (ICIT)*, IEEE, 2021, pp. 799–804. doi: 10.1109/ICIT52682.2021.9491752
- [51] N. Tajbakhsh *et al.*, "Convolutional Neural Networks for Medical Image Analysis: Full Training or Fine Tuning?," *IEEE Trans Med Imaging*, vol. 35, no. 5, pp. 1299–1312, May 2016, doi: 10.1109/TMI.2016.2535302.



- [52] M. A. Islam, S. I. Rashid, N. U. I. Hossain, R. Fleming, and A. Sokolov, “An integrated convolutional neural network and sorting algorithm for image classification for efficient flood disaster management,” *Decision Analytics Journal*, vol. 7, p. 100225, 2023. doi: 10.1016/j.dajour.2023.100225
- [53] D. Irfan, R. Rosnelly, M. Wahyuni, J. T. Samudra, and A. Rangga, “Perbandingan optimasi sgd, adadelata, dan adam dalam klasifikasi hydrangea menggunakan cnn,” *Journal of Science and Social Research*, vol. 5, no. 2, pp. 244–253, 2022.
- [54] K. He, G. Gkioxari, P. Dollár, and R. Girshick, “Mask r-cnn,” in *Proceedings of the IEEE international conference on computer vision*, 2017, pp. 2961–2969.
- [55] S. Singh and B. K. Tripathi, “Pneumonia classification using quaternion deep learning,” *Multimed Tools Appl*, vol. 81, no. 2, pp. 1743–1764, Jan. 2022, doi: 10.1007/s11042-021-11409-7. doi: 10.1007/s11042-021-11409-7